

DARK MATTER PRODUCTION AT THE LHC FROM BLACK HOLE REMNANTS

*G. C. Nayak*¹

Department of Physics, University of Arizona, Tucson, USA

We study dark matter production at CERN LHC from black hole remnants (BHR). We find that the typical mass of these BHR at the LHC is $\sim 5\text{--}10$ TeV which is heavier than other dark matter candidates, such as axion, axino, neutralino, etc. We propose the detection of this dark matter via single jet production in the process $pp \rightarrow \text{jet} + \text{BHR}$ (dark matter) at CERN LHC. We find that for zero impact parameter partonic collisions, the monojet cross section is not negligible in comparison to the standard model background and is much higher than the other dark matter scenarios studied so far. We also find that $d\sigma/dp_T$ of jet production in this process increases as p_T increases, whereas in all other dark matter scenarios the $d\sigma/dp_T$ decreases at CERN LHC. This may provide a useful signature for dark matter detection at the LHC. However, we find that when the impact parameter dependent effect of inelasticity is included, the monojet cross section from the above process becomes much smaller than the standard model background and may not be detectable at the LHC.

Изучается рождение темной материи из осколков черной дыры на большом адронном коллайдере (ЛХС) в ЦЕРН. Найдено, что типичная масса этих осколков для условий ЛХС порядка 5–10 ТэВ, что тяжелее других кандидатов для темной материи, таких как аксион, аксино, нейтрино и др. Предлагается детектировать эти осколки на ЛХС в ЦЕРН через рождение одиночных струй в процессе $pp \rightarrow \text{струя} + \text{осколок черной дыры}$ (темная материя). Показано, что для партонных соударений с нулевым прицельным параметром сечение рассеяния одиночной струи непренебрежимо мало по сравнению с фоном стандартной модели и гораздо больше, чем в иных сценариях рождения темной материи, изученных до сих пор. Также показано, что в этом процессе $d\sigma/dp_T$ рождения струи растет с ростом p_T , в то время как все другие сценарии рождения темной материи предсказывают падение $d\sigma/dp_T$ для ЛХС в ЦЕРН. Такое поведение может служить полезной сигнатурой для детектирования темной материи на ЛХС. В то же время мы нашли, что если учесть неупругие процессы, зависящие от прицельного параметра, то сечение рассеяния одиночной струи для рассмотренного процесса становится гораздо меньше, чем фон стандартной модели, и может быть не детектируемо на ЛХС.

PACS: 95.35.+d; 04.50.Gh; 04.70.Dy; 13.85.-t

By now it is confirmed that dark matter exists and it consists of a large fraction of the energy density of the universe ($\sim 25\%$) [1], while dark energy consists of $\sim 70\%$. The energy density of the nonbaryonic dark matter in the universe is known to be [2]

$$\Omega_{\text{DM}} h^2 = 0.112 \pm 0.009, \quad (1)$$

¹E-mail: nayak@physics.arizona.edu

where Ω_{DM} is the energy density in units of the critical density and $h \sim 0.71$ is the normalized Hubble parameter. Since the visible matter consists of only $\sim 5\%$ of the matter of the universe, the laws of physics or laws of gravity, as we know today, may not be sufficient to explain the dark matter and dark energy content of the universe.

One of the challenges we face today is to identify the nonbaryonic weakly interacting massive particle (WIMP) or WIMP-like particle which consists of dark matter [3]. Identification of this WIMP or WIMP-like dark matter candidate is one of the outstanding questions in basic science today. At present, the possible proposals include axion, axino, neutralino, gravitino and black hole remnants, etc. [4]. Black hole remnants as a source of dark matter is studied in various inflation models in [4–6]. These black hole remnants are from black holes which were produced due to the density perturbations in the early universe during inflation.

An exciting possibility is that black hole remnants (BHR) that make up some or all of dark matter may be produced at high-energy colliders such as the Large Hadron Collider (LHC) at CERN. Such prospects are particularly promising because both ATLAS and CMS detectors at the LHC will search for black holes. In this paper we study dark matter production from black hole remnants at CERN LHC.

The Schwarzschild radius of $d(= n + 4)$ -dimensional black hole is given by

$$R_{\text{BH}} = w_n \frac{1}{M_P} \left(\frac{M_{\text{BH}}}{M_P} \right)^{\frac{1}{n+1}}, \quad w_n = \left(\frac{16\pi}{(n+2)\Omega_{n+3}} \right)^{\frac{1}{n+1}}, \quad (2)$$

where M_{BH} is the black hole mass and M_P is the Planck mass of $\sim \text{TeV}$ at the LHC [7]. The Hawking temperature of the black hole becomes

$$T_{\text{BH}} = \frac{n+1}{4\pi R_{\text{BH}}}. \quad (3)$$

Once black hole is produced at the LHC, it will emit particles due to Hawking radiation [8]. However, in the absence of a theory of quantum gravity it is not clear what happens to black hole radiation when its mass approaches Planck mass. It is commonly believed that quantum gravity implies the existence of a minimum length [9] which leads to a modification of the quantum mechanical uncertainty principle

$$\Delta x \geq \frac{\hbar}{\Delta p} \left[1 + \left(\alpha' L_P \frac{\Delta p}{\hbar} \right)^2 \right], \quad (4)$$

where L_P is the Planck length and α' is a dimensionless constant ~ 1 which depends on the details of the quantum gravity theory. The generalized uncertainty principle (GUP), Eq. (4), can be derived in the context of noncommutative quantum mechanics [10], string theory [11] or from minimum length considerations [12].

If we implement GUP and demand that the position uncertainty Δx of the produced particle from the black hole is of the order of Schwarzschild radius, then the modified temperature of the black hole becomes [6, 13]

$$T_{\text{BHR}} = 2T_{\text{BH}} \left[1 + \sqrt{1 - \frac{1}{w_n^2 \left(\frac{M_{\text{BH}}}{M_P} \right)^{\frac{2}{n+1}}}} \right]^{-1}. \quad (5)$$

The black hole temperature is undefined for $M_{\text{BH}} < M_{\text{min}}$, where

$$M_{\text{min}} = \frac{n+2}{8\Gamma\left[\frac{n+3}{2}\right]} \pi^{\frac{n+1}{2}} M_P. \quad (6)$$

Black holes with mass less than M_{min} do not exist, since their horizon radius would fall below the minimum allowed length. Hence, Hawking evaporation must stop once the black hole mass reaches M_{min} . This creates a black hole remnant of mass M_{min} which is of $\sim \text{TeV}$ at the LHC. Since this black hole remnant is weakly interacting and heavy, it is a possible candidate for dark matter at the LHC [5, 6].

Since the dark matter is weakly interacting, it cannot be directly detected at the LHC. For this purpose we will study dark matter production from black hole remnants (BHR) at the LHC in the process $pp \rightarrow \text{jet} + \text{BHR}$ (dark matter). We propose indirect detection of dark matter via single jet measurement in the above process $pp \rightarrow \text{jet} + \text{BHR}$ (dark matter) at the LHC. The emission rate dN/dt [14] for jet production with momentum/energy $E = |\mathbf{p}|$ from a black hole, which becomes a black hole remnant of mass M_{min} after time t_f , is given by

$$\frac{dN}{d^3p} = \int_0^{t_f} \frac{c_s \sigma_s}{32\pi^3} \frac{dt}{\left[\exp\left(\frac{E}{T_{\text{BHR}}}\right) \pm 1\right]}, \quad (7)$$

where σ_s is the d -dimensional grey body factor [15]; T_{BHR} is the GUP implemented black hole temperature as given by Eq.(5); t_f is the decay time [13], and c_s is the multiplicity factor. The sign \pm is for quark and gluon jets, respectively.

This result in Eq.(7) is for jet production from a single black hole of temperature T_{BHR} (with a black hole remnant of mass M_{min}). To obtain total jet cross section from this process, we need to multiply the number of jets produced from a single black hole with the total black hole production cross section in pp collisions at the LHC.

The black hole production cross section in pp collisions at $\sqrt{s} = 14 \text{ TeV}$ at the LHC is given by [8]

$$\sigma_{\text{BH}}^{pp \rightarrow \text{BH}} = \sum_{ij} \int_{\tau}^1 dx_i \int_{\tau/x_i}^1 dx_j f_{i/p}(x_i, Q^2) \times f_{j/p}(x_j, Q^2) \hat{\sigma}^{ij \rightarrow \text{BH}}(\hat{s}) \delta(x_i x_j - M_{\text{BH}}^2/s), \quad (8)$$

In this expression $\hat{\sigma}^{ab \rightarrow \text{BH}}(\hat{s}) = \pi R_{\text{BH}}^2$ is the black hole production cross section in partonic collisions at zero impact parameter; $x_i(x_j)$ is the longitudinal momentum fraction of the parton inside the proton at the LHC, and $\tau = M_{\text{BH}}^2/s$. Energy-momentum conservation implies $\hat{s} = x_i x_j s = M_{\text{BH}}^2$. We use $Q = 1/R_{\text{BH}}$ as the factorization scale at which the parton distribution functions are measured. \sum_{ij} represents the sum over all partonic contributions

where $i, j = q, \bar{q}, g$.

The above formula, Eq.(8), is valid for zero impact parameter partonic collisions. To include the impact parameter dependent effect of inelasticity, we adopt the impact parameter

b weighted average of the inelasticity used in [16]

$$\sigma_{\text{BH}}^{pp \rightarrow \text{BH}} = \sum_{ij} \int_0^1 2z dz \int_{\frac{(x_{\text{min}} M_P)^2}{y^2(z)s}}^1 du \int \frac{dv}{v} f_{i/p}(v, Q^2) \times$$

$$\times f_{j/p}(u/v, Q^2) \hat{\sigma}^{ij \rightarrow \text{BH}}(M_{\text{BH}} = \sqrt{us}), \quad (9)$$

where $z = b/b_{\text{max}}$. The partonic level cross section is given by [17]

$$\hat{\sigma}^{ij \rightarrow \text{BH}}(M_{\text{BH}} = \sqrt{us}) = F(n) \pi R_S^2, \quad (10)$$

where

$$R_S = \frac{1}{M_P} \left[\frac{2^n \pi^{\frac{n-3}{2}} \Gamma\left[\frac{n+3}{2}\right] \sqrt{us}}{n+2} \frac{\sqrt{us}}{M_P} \right]^{\frac{1}{n+1}}. \quad (11)$$

The inelasticity parameter $y(z)$ and the cross-section correction factor $F(n)$ are taken from [18]. We use the factorization scale $Q = 1/R_S$ at which the parton distribution functions are measured. $x_{\text{min}} = M_{\text{BH}}^{\text{min}}/M_P$, where $M_{\text{BH}}^{\text{min}}$ is the smallest black hole mass for which we trust semiclassical calculation.

The total jet production cross section in the process $pp \rightarrow \text{jet} + \text{BHR}$ (dark matter) at the LHC is then given by

$$\sigma = N \times \sigma_{\text{BH}}, \quad (12)$$

where σ_{BH} is given by Eq. (8). To obtain p_T distribution we use $d^3p = 2\pi dp_T p_T^2 dy \cosh y$ in Eq. (7); y is the rapidity.

In our calculation we use CTEQ6M parton distribution functions inside the proton [19]. The number of extra dimensions is chosen to be $n = 6$ so that we do not rule out the possibility of Planck mass $M_P = 1$ TeV [20]. Since initial mass of the black hole must be greater than the Planck mass, we choose $M_i^{\text{BH}} = 5M_P$ in our calculation. It can be seen from Eq. (6) that the black hole remnant mass M_{min} does not depend on the black hole mass but depends on the Planck mass and number of extra dimensions. We find that the typical black hole remnant mass $M_{\text{min}} = 4.7$ TeV for $M_P = 1$ TeV and $M_{\text{min}} = 9.7$ TeV for $M_P = 2$ TeV at the LHC.

For a comparison we list here the lower limits on the Planck mass M_P by various collider experiments. The current limits from LEP2, CDF (run II) and D0 (run II) are as follows. The LEP2 analysis has set a lower limit on the Planck mass $M_P^{\text{min}} = 1.69$ TeV by using graviton production [21]. Search for large extra dimensions in the production of jets and missing transverse energy at CDF gives $M_P^{\text{min}} = 0.83$ TeV for $n = 6$ to $M_P^{\text{min}} = 1.18$ TeV for $n = 2$ [22], where n is the number of extra dimensions. The search for large extra dimensions in final states containing one photon or jet and large missing transverse energy at CDF gives $M_P^{\text{min}} = 0.94$ TeV for $n = 6$ to $M_P^{\text{min}} = 1.4$ TeV for $n = 2$ [23]. Dielectron and diphoton measurements at D0 gives $M_P^{\text{min}} = 1.3$ TeV for $n = 7$ to $M_P^{\text{min}} = 2.1$ TeV for $n = 2$ [24]. Search for large extra dimensions via single photon plus missing energy at D0 sets the limit $M_P^{\text{min}} = 0.778$ TeV for $n = 8$ to $M_P^{\text{min}} = 0.884$ TeV for $n = 2$ [25].

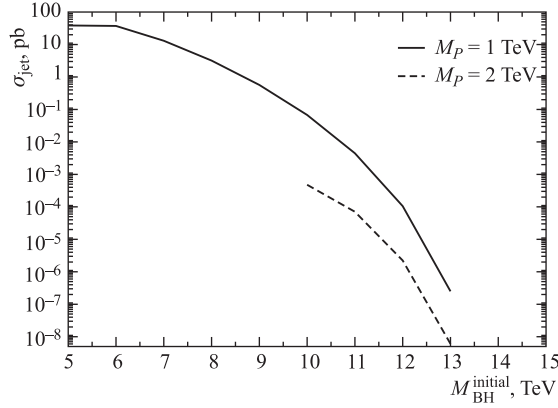


Fig. 1. Total cross section for monojet production in the process $pp \rightarrow \text{jet} + \text{BHR}$ (dark matter) at the LHC at $\sqrt{s} = 14$ TeV

In Fig. 1 we present the monojet cross section, in the process $pp \rightarrow \text{jet} + \text{BHR}$ (dark matter), as a function of initial black hole mass at CERN LHC. This result is for zero impact parameter partonic collisions. The solid line is for Planck mass 1 TeV and the dashed line is for Planck mass 2 TeV. It can be seen that for Planck mass 1 TeV and initial black hole mass 5 TeV the monojet cross section, in the process $pp \rightarrow \text{jet} + \text{BHR}$ (dark matter), is 38.5 pb. This value is much higher than the cross section 18.6 fb obtained in other dark matter scenario with dark matter mass ~ 100 GeV [26]. In our case the dark matter mass (BHR mass) is 4.7 TeV, which is much heavier than 100 GeV dark matter mass used in [26].

This is very exciting because we have found a heavier dark matter candidate at the LHC with larger cross section. This is due to the fact that the temperature of a typical black hole formed at the LHC is $\sim \text{TeV}$. Hence, jets produced from black holes at such a high temperature is large. On the other hand, in other dark matter scenarios the jet plus dark matter production is via direct parton collisions and hence the cross section is small. Also, unlike [26], our dark matter signal is not negligible in comparison to the standard model background. A typical standard model background is ~ 130 pb for $p_T^{\text{min}} = 100$ GeV and 1300 pb for $p_T^{\text{min}} = 30$ GeV. In our case the cross section is ~ 40 pb, whereas in case of [26] the cross section is 18.6 fb.

In Fig. 2 we present the p_T distribution of the jet production cross section, in the process $pp \rightarrow \text{jet} + \text{BHR}$ (dark matter), at CERN LHC at $\sqrt{s} = 14$ TeV. This result is for zero impact parameter partonic collisions. The solid line is for Planck mass equal to 1 TeV and the dashed line is for Planck mass equal to 2 TeV. It can be seen that $d\sigma/dp_T$ of jet, from the process $pp \rightarrow \text{jet} + \text{BHR}$ (dark matter), increases as p_T increases. This is in contrast to all other dark matter scenarios where $d\sigma/dp_T$ decreases as p_T increases. This is also in contrast to all standard model processes where $d\sigma/dp_T$ decreases as p_T increases.

This is explained in detail in [27] and can be understood as follows. From the emission rate dN/dt in Eq. (7) we find

$$\frac{dN}{dp_T} = 2\pi p_T^2 \int dy \cosh y \int_0^{t_f} \frac{c_s \sigma_s}{32\pi^3} \left[\frac{dt}{\exp\left(\frac{p_T \cosh y}{T_{\text{BHR}}}\right) \pm 1} \right]. \quad (13)$$

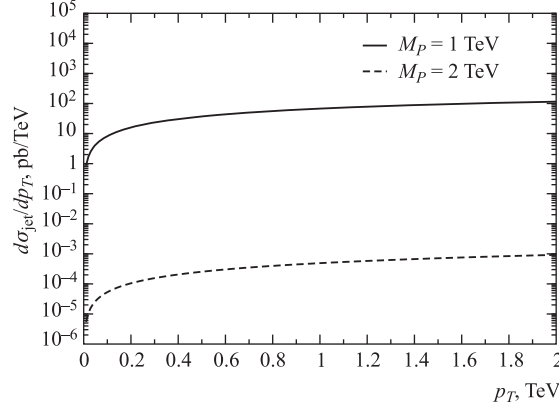


Fig. 2. p_T differential cross section for monojet production in the process $pp \rightarrow \text{jet} + \text{BHR}$ (dark matter) at the LHC at $\sqrt{s} = 14$ TeV

Since the temperature of the black hole remnant $T_{\text{BHR}} \sim 1\text{--}2$ TeV at the LHC, the thermal distribution $\frac{1}{\left[\exp\left(\frac{p_T \cosh y}{T_{\text{BHR}}}\right) \pm 1 \right]}$ remains almost flat with respect to p_T as long as p_T is

not much larger than T_{BHR} . Hence, the increase of $d\sigma/dp_T$ as p_T increases comes from the increase in the transverse momentum phase space factor p_T^2 , as can be seen from Eq.(13). For very large value of $p_T \gg 2$ TeV, the $d\sigma/dp_T$ will of course start decreasing. Hence, the increase of $d\sigma/dp_T$ as p_T increases may provide a unique signal for dark matter detection from black hole remnants at CERN LHC.

In Fig. 3 we present the results which include the impact parameter dependent effect of inelasticity in the cross section (see Eq.(9)). We present the monojet cross section, in the process $pp \rightarrow \text{jet} + \text{BHR}$ (dark matter), as a function of x_{min} at CERN LHC. The solid line is for Planck mass 1 TeV and the dashed line is for Planck mass 1.5 TeV. The monojet cross section is very small for $M_P = 2$ TeV and hence we do not report it. It can be seen

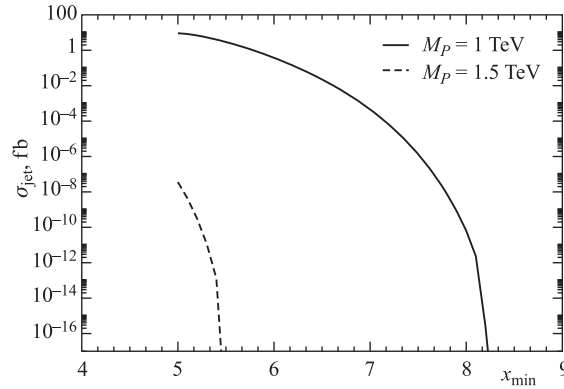


Fig. 3. Total cross section for monojet production in the process $pp \rightarrow \text{jet} + \text{BHR}$ (dark matter) at the LHC at $\sqrt{s} = 14$ TeV which includes the effect of inelasticity

that for Planck mass equal to 1 TeV and x_{\min} equal to 5, the monojet cross section, in the process $pp \rightarrow \text{jet} + \text{BHR}$ (dark matter), is 10 fb which is much smaller than the zero impact parameter case (see Fig. 1). Hence, when the impact parameter weighted average of the inelasticity is included, the monojet cross section becomes much smaller than the standard model background and may not be detectable at the LHC.

In Fig. 4 we present the p_T distribution of the cross section which includes the impact parameter dependent effect of inelasticity (see Eq. (9)). We use $x_{\min} = 5$ in our calculation. The solid line is for Planck mass equals to 1 TeV and the dashed line is for Planck mass equal to 1.5 TeV. The monojet cross section is very small for $M_P = 2$ TeV and hence we do not report it. It can be seen that $d\sigma/dp_T$ of jet, from the process $pp \rightarrow \text{jet} + \text{BHR}$ (dark matter), increases as p_T increases. However, this cross section is much smaller than the standard model background and may not be detectable at the LHC. Only for zero impact parameter partonic collisions, the cross section becomes comparable to the standard model predictions (see Fig. 2).

Finally, we make some comments on the energy loss from a black hole to become a black hole remnant and the TeV scale jets. For $M_P = 1$ TeV and $M_{\text{BH}} = 5$ TeV, the mass of the black hole remnant is $M_{\text{BHR}} = 4.7$ TeV. Similarly for $M_P = 2$ TeV and $M_{\text{BH}} = 10$ TeV, the mass of the black hole remnant is $M_{\text{BHR}} = 9.7$ TeV. Hence, in both the cases the energy loss from a black hole to become a black hole remnant is 300 GeV. One might wonder how can one compute high- p_T (~ 2 TeV) jets from black hole remnants in Figs. 2 and 4. This is due to very high temperature of the black hole remnants. For $M_P = 1$ TeV, $M_{\text{BH}} = 5$ TeV and $M_{\text{BHR}} = 4.7$ TeV, the temperature of the black hole remnant is $T_{\text{BHR}} = 0.98$ TeV, which can be easily checked from Eqs. (2), (3) and (5). For $M_P = 2$ TeV, $M_{\text{BH}} = 10$ TeV and $M_{\text{BHR}} = 9.7$ TeV, the temperature of the black hole remnant is $T_{\text{BHR}} = 1.96$ TeV. Hence, the high- p_T jets in Figs. 2 and 4 are due to very high temperatures ($T_{\text{BHR}} \sim 1\text{--}2$ TeV) of the black hole remnants.

To conclude, we have studied dark matter production at CERN LHC from black hole remnants (BHR). We have found that the typical mass of these BHR at the LHC is $\sim 5\text{--}10$ TeV, which is heavier than other dark matter candidates, such as axion, axino, neutralino, etc. We have proposed the detection of this dark matter via single jet production in the process

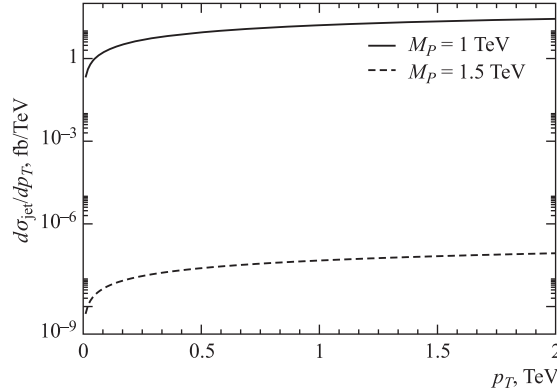


Fig. 4. p_T differential cross section for monojet production in the process $pp \rightarrow \text{jet} + \text{BHR}$ (dark matter) at the LHC at $\sqrt{s} = 14$ TeV which includes the inelasticity

$pp \rightarrow \text{jet} + \text{BHR (dark matter)}$ at CERN LHC. We have found that for zero impact parameter partonic collisions, the monojet cross section is not negligible in comparison to the standard model background and is much higher than the other dark matter scenarios studied so far. We have also found that $d\sigma/dp_T$ of jet production in this process increases as p_T increases, whereas in all other dark matter scenarios the $d\sigma/dp_T$ decreases at CERN LHC. This may provide a useful signature for dark matter detection at the LHC. However, we have also shown that, when the impact parameter dependent effect of inelasticity is included, the monojet cross section from the above process becomes much smaller than the standard model background and may not be detectable at the LHC.

Acknowledgements. This work was supported in part by the Department of Energy under contracts DE-FG02-91ER40664, DE-FG02-04ER41319 and DE-FG02-04ER41298.

REFERENCES

1. Zwicky F. // *Helv. Physica Acta*. 1933. V. 6. P. 110; *Astrophys. J.* 1937. V. 86. P. 217;
Rubin V., Ford W.K. // *Astrophys. J.* 1970. V. 159. P. 359;
Rubin V., Thonnard N., Ford W.K. // *Astrophys. J.* 1980. V. 238. P. 471;
Conley A. et al. // *Astrophys. J.* 2006. V. 644. P. 1;
Spergel D. N. et al. (*WMAP Collab.*) // *Astrophys. J. Suppl.* 2007. V. 170. P. 377.
2. Spergel D. N. et al. (*WMAP Collab.*) // *Astrophys. J. Suppl. Ser.* 2003. V. 148. P. 175.
3. Gondolo P. astro-ph/0403064.
4. Rajagopal K., Turner M. S., Wilczek F. // *Nucl. Phys. B*. 1991. V. 358. P. 447;
Feldman D., Nath P. // *Phys. Lett. B*. 2008. V. 662. P. 190;
Baer H., Tata X. hep-ph/0805.1905;
Arkani-Hamed N., Weiner N. // *JHEP*. 2008. V. 0812. P. 104;
Arrwonitt R. et al. hep-ph/0701053;
Ellis J. R., Raklev A. R., Oye O. K. // *JHEP*. 2006. V. 0610. P. 061;
Kitano R., Nomura Y. // *Phys. Lett. B*. 2006. V. 632. P. 162;
Drees M. et al. // *Phys. Rev. D*. 2001. V. 63. P. 035008;
Birkedal A., Matchev K., Perelstein M. // *Phys. Rev. D*. 2004. V. 70. P. 077701;
Feng J. L., Rajaraman A., Takayama F. // *Phys. Rev. Lett.* 2003. V. 91. P. 011302.
5. Baumann D., Steinhardt P., Turok N. hep-th/0703250.
6. Chen P. // *New Astron. Rev.* 2005. V. 49. P. 233; *Nucl. Phys. B (Proc. Suppl.)*. 2003. V. 124. P. 103.
7. Arkani-Hamed N., Dimopoulos S., Dvali G.R. // *Phys. Lett. B*. 1998. V. 429. P. 263; *Phys. Rev. D*. 1999. V. 59. P. 086004;
Antoniadis I. et al. // *Phys. Lett. B*. 1998. V. 436. P. 257;
Randall L., Sundrum R. // *Phys. Rev. Lett.* 1999. V. 83. P. 3370; 4690;
Banks T., Fischler W. hep-th/9906038.
8. Dimopoulos S., Landsberg G. // *Phys. Rev. Lett.* 2001. V. 87. P. 161602;
Argyres P. C., Dimopoulos S., March-Russell J. // *Phys. Lett. B*. 1998. V. 441. P. 96;
Giddings S. B., Thomas S. // *Phys. Rev. D*. 2002. V. 65. P. 056010;
Anchordoqui L., Goldberg H. // *Ibid.* P. 047502; *Phys. Rev. D*. 2003. V. 67. P. 064010;
Chamblin A., Nayak G. C. // *Phys. Rev. D*. 2002. V. 66. P. 091901;
Feng J. L., Shapere A. D. // *Phys. Rev. Lett.* 2002. V. 88. P. 021303;
Chamblin A., Cooper F., Nayak G. C. // *Phys. Rev. D*. 2004. V. 70. P. 075018;

- Cheung K.* // *Phys. Rev. Lett.* 2002. V. 88. P. 221602;
Koch B. et al. // *JHEP.* 2005. V. 0510. P. 053;
Humanic T. J. et al. // *Intern. J. Mod. Phys. E.* 2007. V. 16. P. 841–852;
Cavaglia M. et al. // *Comp. Phys. Commun.* 2007. V. 177. P. 506–517;
Cavaglia M. et al. // *JHEP.* 2007. V. 0706. P. 055;
Gingrich D. M. // *Ibid.* V. 0711. P. 064.
9. *Garay L. J.* // *Intern. J. Mod. Phys. A.* 1995. V. 10. P. 145; gr-qc/9403008.
 10. *Maggiore M.* // *Phys. Rev. D.* 1994. V. 49. P. 5182; hep-th/9305163; *Phys. Lett. B.* 1993. V. 319. P. 83; hep-th/9309034.
 11. *Amati D., Ciafaloni M., Veneziano G.* // *Phys. Lett. B.* 1989. V. 216. P. 41; *Nucl. Phys. B.* 1990. V. 347. P. 550; 1993. V. 403. P. 707;
Konishi K., Paffuti G., Provero P. // *Phys. Lett. B.* 1990. V. 234. P. 276.
 12. *Maggiore M.* // *Phys. Lett. B.* 1993. V. 304. P. 65; hep-th/9301067.
 13. *Cavaglia M., Das S.* // *Class. Quant. Grav.* 2004. V. 21. P. 4511;
Cavaglia M., Das S., Maartens R. // *Class. Quant. Grav.* 2003. V. 20. P. L205.
 14. *Han T., Kribs G. D., McElrath B.* // *Phys. Rev. Lett.* 2003. V. 90. P. 031601.
 15. *Kanti P., March-Russell J.* // *Phys. Rev. D.* 2002. V. 66. P. 024023; 2003. V. 67. P. 104019;
Ida D., Oda K., Park S. C. // *Ibid.* P. 064025.
 16. *Meade P., Randall L.* hep-ph/0708.3017.
 17. *Anchordoqui L. A. et al.* // *Phys. Lett. B.* 2004. V. 594. P. 363.
 18. *Yoshino H., Rychkov V. S.* // *Phys. Rev. D.* 2005. V. 71. P. 104028.
 19. *Pumplin J. et al.* // *JHEP.* 2002. V. 0207. P. 102.
 20. *Anchordoqui L. A. et al.* // *Phys. Rev. D.* 2003. V. 68. P. 104025;
Abbott B. et al. (D0 Collab.) // *Phys. Rev. Lett.* 2001. V. 86. P. 1156;
Abazov V. M. et al. (D0 Collab.) // *Phys. Rev. Lett.* 2003. V. 90. P. 251802;
Hagiwara K. et al. (Particle Data Group Collab.) // *Phys. Rev. D.* 2002. V. 66. P. 01001.
 21. *Abdallah J. et al. (DELPHI Collab.)* // *Eur. Phys. J. C.* 2009. V. 60. P. 17–23; hep-ex/0901.4486.
 22. *Abulencia A. et al. (CDF Collab.)* // *Phys. Rev. Lett.* 2006. V. 97. P. 171802; hep-ex/0605101.
 23. *Aaltonen T. et al. (CDF Collab.)* // *Phys. Rev. Lett.* 2008. V. 101. P. 181602; arXiv:0807.3132.
 24. *Abazov V. M. et al. (D0 Collab.)* // *Phys. Rev. Lett.* 2009. V. 102. P. 051601; hep-ex/0809.2813.
 25. *Abazov V. M. et al. (D0 Collab.)* // *Phys. Rev. Lett.* 2008. V. 101. P. 011601; hep-ex/0803.2137.
 26. *Feng J. L., Su S., Takayama F.* // *Phys. Rev. Lett.* 2006. V. 96. P. 151802.
 27. *Nayak G. C., Smith J.* // *Phys. Rev. D.* 2006. V. 74. P. 014007; *Haunting Higgs Boson in Mini Black Holes* // *New Scientist.* 2006. Iss. 2562. P. 12.

Received on July 6, 2010.